The Astrophysical Journal, 235:163–176, 1980 January 1

SOFT X-RAY PULSATIONS FROM SS CYGNI

F. A. Córdova, T. J. Chester, I. R. Tuohy, and G. P. Garmire
California Institute of Technology, Pasadena
Received 1979 April 20; accepted 1979 July 18

ABSTRACT

Pulsed soft X-rays (0.1–0.5 keV) with a period of 9 s and a pulsed fraction that varies between 0 and 100% were detected from the dwarf nova SS Cygni at the peak of an optical outburst. This detection confirms for the first time the supposed high-energy origin of optical pulsations seen in erupting dwarf novae. The pulse shape is remarkably sinusoidal for such a large amplitude oscillation. The X-ray pulsation observed in this outburst is not coherent, in contrast to previous claims for the related optical oscillations. Instead, the *phase* of the pulsation apparently executes a random walk with a Q of ~ 25, whereas the *period* is quite stable: $\dot{P} \sim -1 \times 10^{-5}$ s s^{-1}. There is no evidence for any other periodic behavior on time scales between 160 ms and 3 hr. A blackbody fit to the observed spectrum yields $T \sim 3.5 \times 10^5$ K and a flux at the Earth of $\sim 4.5 \times 10^{-11}$ ergs cm^{-2} s^{-1} in the $\frac{1}{4}$ keV band. This in turn implies a total luminosity (integrated over all frequencies) at the source of $\sim 1.8 \times 10^{33} \times (d/200 \text{ pc})^2$ ergs s^{-1}. Previous models for the optical oscillations fail to account for the properties of the X-ray pulsation. It is possible that an as yet unspecified instability in the boundary layer between the white dwarf and the accretion disk is the origin of the pulsation.

Subject headings: stars: dwarf novae — stars: individual — X-rays: binaries

I. INTRODUCTION

Although our understanding of dwarf novae has progressed rapidly in the last 20 years, some of the most fundamental facts remain unexplained. (For general reviews of cataclysmic variables, see Warner 1976; Bath 1976; Robinson 1976; Bath 1978.) This situation can be largely traced to our ignorance regarding the basic process that fuels the observed luminosity in these close binary systems; that is, we do not know the precise manner in which mass is transferred from the red star via the accretion disk to the surface of the white dwarf.

Like many other dwarf novae, SS Cygni shows low-amplitude, short-period optical pulsations during outbursts. For SS Cyg, periods ranging from 8.5 to 10.6 s have been measured (Patterson, Robinson, and Kiplinger 1978; Horne and Gomer 1979; Patterson 1979). The optical pulsations are thought to be reprocessed pulsed X-ray or EUV emission produced in the vicinity of the compact star (Warner and Brickhill 1978), although the origin of the pulsation itself remains unclear. It was hoped that high-energy observations could test this hypothesis.

Hard X-rays (2–25 keV) have been detected from SS Cyg during optical quiescence by *HEAO 1* with a flux of 1.6×10^{-10} ergs cm^{-2} s^{-1} (Mason, Córdova, and Swank 1979). It is unlikely, though, that hard X-rays are the source of the optical pulsation. Swank (1979) reports a 90% confidence limit to the pulsed fraction of SS Cyg during quiescence of $\sim 2\%$ for periods consistent with those of the optical pulsations. In addition, the hard X-ray flux *decreases* during eruption (Ricketts, King, and Raine 1979). During the outburst described herein there was a residual hard X-ray flux of $\sim 4 \times 10^{-11}$ ergs cm^{-2} s^{-1}; the preliminary upper limit to a hard X-ray pulsation during this outburst is $\sim 6\%$ (Swank 1979).

In soft X-rays (0.1–0.5 keV), on the other hand, there is an *increase* in intensity during outbursts by about an order of magnitude. Our own *HEAO 1* pointing observation of SS Cyg on 1977 December 12 during quiescence gives an upper limit of 5×10^{-12} ergs cm^{-1} s^{-1}. This is consistent with the marginal detection of $\frac{1}{4}$ keV X-rays from SS Cyg during quiescence by Heise *et al.* (1978). During outbursts, however, soft X-rays and EUV from SS Cyg have been detected with an average flux of 5×10^{-11} ergs cm^{-2} s^{-1} by several experimenters (Rappaport *et al.* 1974; Hearn, Richardson, and Li 1976; Margon *et al.* 1978). The observed correlation between soft X-ray and optical brightenings made it important to search for soft X-ray pulsations during eruptions.

In 1978 June we were fortunately able to point *HEAO 1* at SS Cyg during an outburst. This was the first X-ray pointing at an erupting dwarf nova, and hence the first experiment capable of looking for rapid X-ray variability during a maximum. The soft X-rays from SS Cyg were indeed highly modulated at a period close to observed optical periods in the object, confirming the soft X-rays as the ultimate source of the optical pulsations. The large amplitude allowed us to study the properties of the pulsation in detail.

This paper is organized as follows: in § II we present the soft X-ray observations from this pointing; § III is devoted to a detailed analysis of the pulsation; § IV includes a discussion of possible models for the origin and nature of the pulsation; and § V is a summary of the implications of this analysis for future investigations.

II. THE OBSERVATIONS

On 1978 June 13 *HEAO 1* investigators were alerted by the American Association of Variable Star Observers that SS Cyg was undergoing an optical outburst. A *HEAO 1* pointing at SS Cyg commenced June 14.8 UT and lasted ~6 hr. The inset in Figure 1 displays the visual light curve and shows that the satellite observation took place near the peak of the outburst. We reproduce in Figure 1 a representative portion of the X-ray data, showing the large amplitude pulsations with a period of ~9 s.

a) *The Instrumentation*

The low energy detector LED 1 of the A-2 experiment[1] on *HEAO 1* was used for this observation. A complete description of the experiment is given in Rothschild *et al.* (1979). Briefly, LED 1 is a gas proportional counter with sensitivity in the range 0.1–3 keV. The collimator in front of the detector has a 3° FWHM field of view along the satellite meridian, and coaligned fields of view of 1°.5 and 3° FWHM along the satellite azimuth. The data from both fields of view, representing a combined geometrical area of 380 cm^2, were used for this analysis. All of the data were taken with a time resolution of at least 1.28 s; portions of the observation had 80 ms resolution.

[1] The A-2 experiment of *HEAO 1* is a collaborative effort led by E. Boldt of Goddard Space Flight Center (GSFC) and G. Garmire of the California Institute of Technology (CIT), with collaborators at CIT, Jet Propulsion Laboratory, University of California at Berkeley, and GSFC.

b) *The X-Ray Light Curve*

We used the ratio of the fields of view to subtract the contribution from the X-ray sky background and found that SS Cyg was detectable only below 0.5 keV. This ratio technique confirmed that the substantial flux in the energy band 0.5–2 keV was due to a background feature, probably associated with the large Cyg X-6 background enhancement (Davidsen *et al.* 1977). SS Cyg is completely resolved spectrally from this feature, which is cut off below 0.5 keV. Thus the data used for the analysis described here are taken only from the interval 0.1–0.5 keV, except as noted. The X-ray sky background in this interval contributed ~45% to the summed count rate from both fields of view.

Figure 2 shows the background-subtracted, aspect-corrected soft X-ray light curve for the entire observation. Each point represents an average over 40.96 s of data. The X-ray signal is interrupted by Earth occultations of the source which last for about one-half of each 90 minute satellite orbit. For convenience in referring later in the text to the disjoint sections of data, the sections are labeled OB1, 2, etc. The few low data points in Figure 2 occur at times when the aspect corrections are large. Spacecraft aspect wandering results in larger uncertainties for the count rates

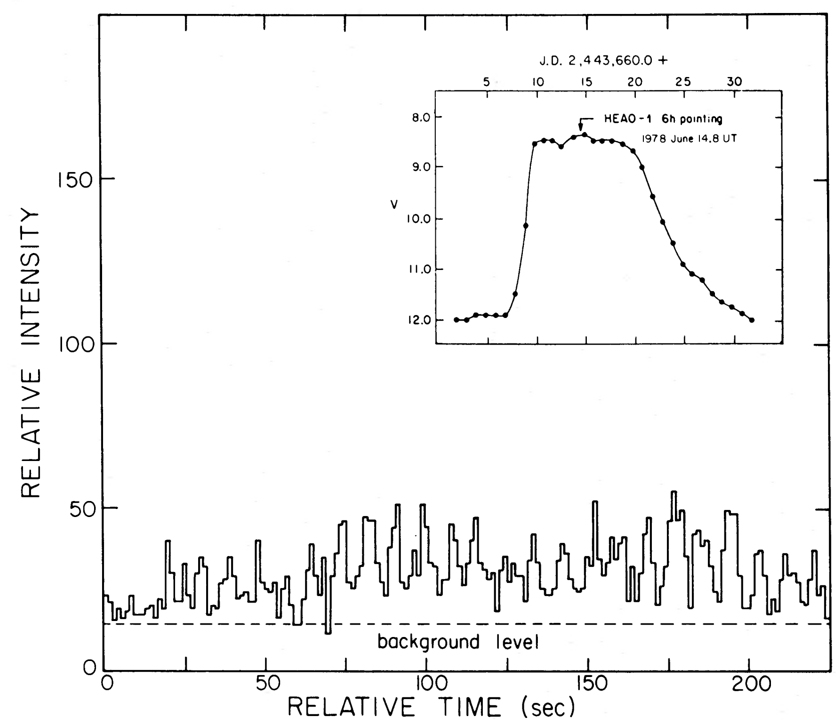

FIG. 1.—A portion of the X-ray data with 1.28 s binning, showing the 9 s pulsations. The dotted line marks the background level. The inset shows the AAVSO visual light curve of SS Cyg for the 1978 June outburst.

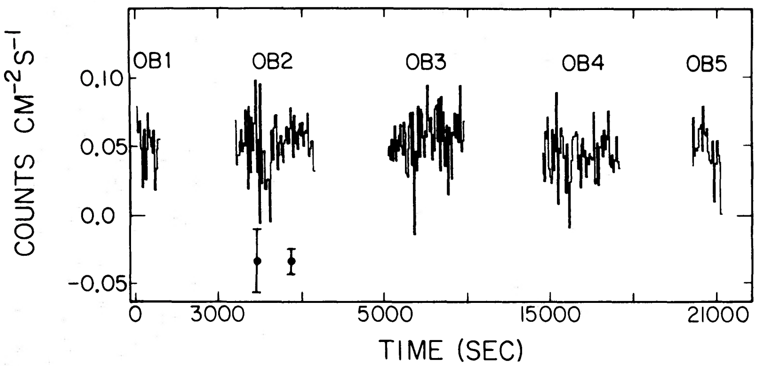

FIG. 2.—The aspect-corrected soft X-ray light curve for the entire SS Cyg pointing. Each point is a 40.96 s average corrected for background by subtracting the different detector fields of view. Dropouts are due to Earth occultation. The satellite orbits are designated OB1, 2, etc., for future reference. Satellite drift motion results in larger uncertainties for the intensities during the first values of OB1, 2, 3, and 4 and the last half of OB5; this is illustrated in the figure by the unequal error bars below OB2.

during the first halves of OB1, 2, 3, and 4, and the last half of OB5 (see representative error bars in Fig. 2). Within the large uncertainties for the individual data points, the amplitude is consistent with being constant during each OB.

Since the data in the first four OBs were taken with the same detector gain, the average count rates from these sections may be compared. The average intensities during OB1, 2, and 3 were 0.045 ± 0.002, 0.045 ± 0.002, and 0.047 ± 0.002 counts cm^{-2} s^{-1}, respectively, while that of OB4 was 0.038 ± 0.001 counts cm^{-2} s^{-1}. Hence the signal from SS Cyg was lower (4 σ) during OB4 by 16%. OB5 was taken with a different detector gain and cannot be compared with the other OBs unless some assumption about the spectrum is made. Assuming the best-fit spectral parameters (see § II*c*), the average intensity of OB5 is $\sim 0.033 \pm 0.002$ counts cm^{-2} s^{-1}. (Any choice of spectral parameters within the 90% confidence limits given in § II*c* will give a value for the intensity of OB5 which is at least as low as the value for OB4.) This apparent monotonic decrease may represent a cooling of the source. Alternatively, the decrease of OB4 and 5 may be correlated with the 6.6 hr binary period of SS Cyg. A longer observation is required to differentiate between these two possibilities. There is no evidence of any periodic modulation of the X-ray intensity on time scales from a few minutes to $\sim$3 hr.

c) *The Spectrum*

We analyzed the SS Cyg pulse-height data taken when the LED 1 high voltage was increased above its nominal value. The higher voltage extended the detector bandpass by reducing the lower threshold from 0.18 keV to 0.13 keV, as determined from an on-board X-ray calibration which immediately followed the SS Cyg observation. Background data for the pointing were derived from data taken while LED 1 was scanning a region of sky close to SS Cyg.

The spectral data below 0.5 keV were parametrized in turn with a blackbody spectrum and a thermal bremsstrahlung spectrum which we approximated with an exponential plus an energy-dependent Gaunt factor (Kellogg, Baldwin, and Koch 1975), allowing for absorption in the interstellar medium (Brown and Gould 1970). The measured flux and the best-fit spectral parameters are given in Table 1. Figure 3 shows the observed count rate spectrum and the best-fit blackbody model, together with the 90% confidence χ^2 contours (using the criterion of Lampton, Margon, and Bowyer 1976) for both types of spectra. From the χ^2 contours, we can set the following limits on the source temperature:

$$5.04 < \log T < 5.82 \quad \text{(blackbody)},$$

$$5.21 < \log T < 6.34 \quad \text{(thermal bremsstrahlung)}.$$

For both models, the upper limit to the column density is 6.3×10^{20} cm^{-2}. The bremsstrahlung model sets a lower limit of 1×10^{19} cm^{-2} on the column density, but in contrast, the blackbody model is consistent with zero column at the 90% confidence level.

TABLE 1

SS CYGNI BEST-FIT SPECTRAL PARAMETERS

Model	Energy (keV)	Flux (ergs cm^{-2} s^{-1})	T (10^5 K)	N_H (10^{20} cm^{-2})	χ^2_ν (23 degrees of freedom)
Blackbody....................	0.13–0.48	$\sim 4.5 \times 10^{-11}$	3.5	1.0	1.4
Thermal bremsstrahlung.......	0.13–0.48	$\sim 4.5 \times 10^{-11}$	4.7	1.4	1.4

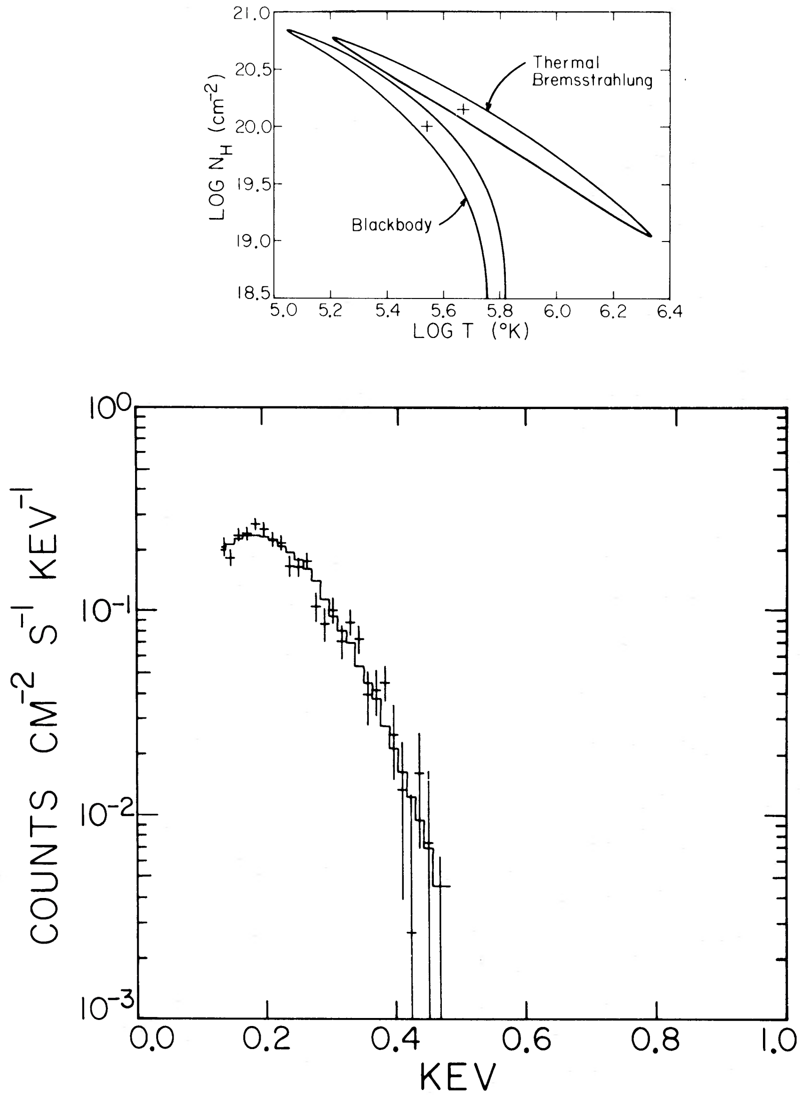

FIG. 3.—The SS Cyg observed spectrum (*crosses*) and the best-fit blackbody model (*solid line*), which represents a kT of 30 eV and a N_H of 1×10^{20} cm^{-2}. The top figure shows the 90% confidence χ^2 contours for both a blackbody and a thermal bremsstrahlung fit.

The best-fit blackbody spectrum of 30 eV yields a *total* luminosity at the source (integrated over all frequencies) of $\sim 1.8 \times 10^{33} \times (d/200 \text{ pc})^2$ ergs s^{-1}. Assuming no interstellar absorption, about 30% of this luminosity is in the energy range accessible to our detector. (The distance of 200 pc is selected as a compromise between various distance estimates; see Warner 1976.) The spectral resolution of the LED 1 proportional counter for energies less than 0.5 keV is $>80\%$, resulting in large uncertainties in the estimation of the temperature (see inset to Fig. 3). Therefore, the best-fit temperature and luminosity derived here should be used only as a guide. In addition, a line emission model may be more appropriate for temperatures of a few $\times 10^5$ K and would systematically increase the temperatures quoted above.

The above spectral data were acquired in a special telemetry mode with a temporal resolution of 20 ms per event. In order to search for possible variability of the source spectrum during the 9 s pulse, we first determined the time of maximum for each pulse (discussed in detail in § III), and superposed each pulse so that the maxima coincided. We then computed a spectral hardness ratio for each of 10 phase bins from the ratio of the (0.23–0.41) to (0.13–0.23) keV count rates. No correlation of the hardness ratio with the sinusoidal pulse light curve was evident; a 2 σ upper limit on a sinusoidal temperature variation (with constant column density) of 70% can be set.

d) *The Pulsations*

The power spectra from discrete Fourier transforms using 1.28 s binning are shown for two of the OBs

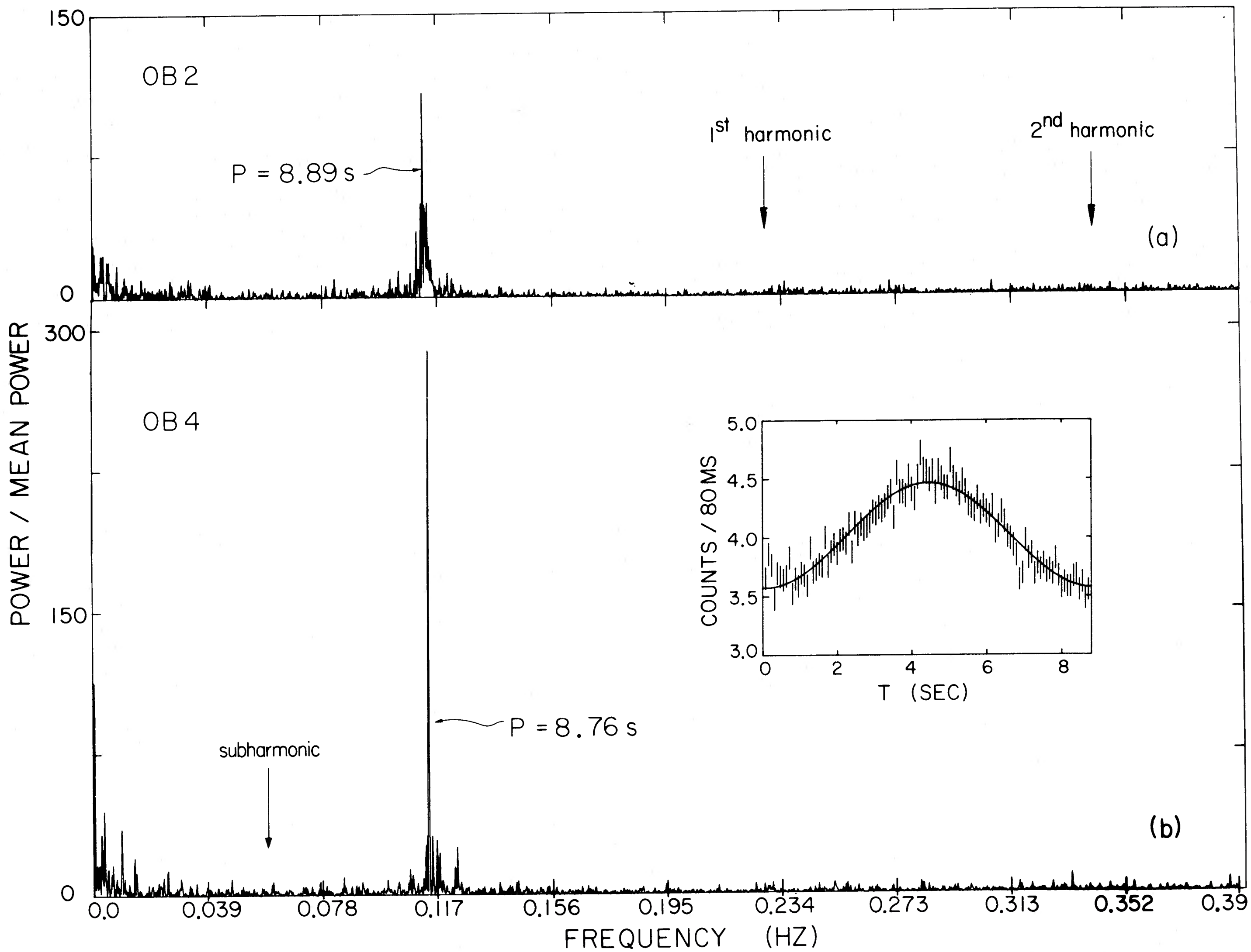

FIG. 4.—Power spectra for OB2 and OB4. The inset in (*b*) shows the superposition of pulses from OB4 and OB5, with all pulses aligned at their peak. The solid line through the pulse profile is the best-fit sinusoid.

in Figure 4. There is an overall period drift evident in the Fourier transforms of $\dot{P} \sim -1 \times 10^{-5}$ s s^{-1} that will be discussed in § III. There are no detectable harmonics or subharmonics of the 9 s period, with a 90% confidence upper limit of 2% of the average X-ray flux. This is only a "formal" upper limit, since the inherent phase jitter (discussed below) of the 9 s pulsation will selectively wash out higher harmonics.

We have analyzed the 80 ms data available for OB4 and OB5 in order to search for pulse structure that might have been smeared out in the Fourier transform by the period variability. Unlike the 1.28 s data for which there is pulse height information, the 80 ms data are integrated over the entire broad-band energy range of 0.1–3 keV. SS Cyg contributes only 30% of the total signal in this band. Superposing 427 pulses so that their maxima coincided resulted in the composite profile shown in Figure 4*b*.

The best-fit sinusoid yields $\chi^2 = 108$ with 106 degrees of freedom, and is shown as a solid line through the pulse profile. Care must be used in deriving upper limits on harmonic amplitudes because spurious harmonics may be introduced in the superposition process. Noise power always increases the fitted pulse amplitude (because amplitudes are always nonnegative) and shifts the observed time of maximum of each pulse. When the pulses are aligned at their peaks, the peak amplitude is thus increased by noise. The amplitudes of other portions of the pulse, however, are progressively reduced by smearing caused by the shifts in the observed time of maximum away from the true peak of each pulse. A complete explanation of this effect is given in Córdova *et al.* (1980).

After allowance for the effects of noise, the 90% confidence upper limit to the amplitudes of harmonics, relative to the fundamental amplitude, is 12% for the first harmonic, and ~7% for the other harmonics. However, the accuracy in the determined time of maximum for each pulse reduces our sensitivity to the harmonics with periods less than ~2.4 s. This remarkably sinusoidal pulse profile is perhaps the simplest pulse profile yet observed in X-ray astronomy.

A Fourier transform of the 80 ms data for OB4 and 5 revealed no excess power at periods between 160 ms and 9 s. We have also searched for power near 0.031 Hz because of the reported quasi-periodic oscillation in visual light at that frequency (Robinson and Nather 1979). Adding the power between 29 and 35 s gives a 90% confidence upper limit to the equivalent pulsed fraction of 2%. Thus we conclude that there is no apparent periodic behavior in SS Cyg, other than the 9 s pulsation, on time scales from 160 ms to 3 hr.

We have employed several techniques in order to examine the short-term behavior of the pulsation. In one type of analysis, short segments of continuous data were folded over many periods in the neighborhood of the 9 s pulsation period, and the amplitudes were plotted as a function of period. The resulting "periodograms" (see Córdova 1979) show a pulsation behavior strikingly similar to the optical pulsations observed from other dwarf novae: large amplitude variability, a long-term period drift, period excursions on short time scales, and the occasional presence of multiple periods. A problem with this type of analysis is that amplitude and/or phase changes can produce sidelobes of the pulsation, creating a false impression of multiple periodic structure. Furthermore, if the pulsation has an overall drift, the segmenting of the data and subsequent folding can create the appearance of discrete periods with a frequency separation correlated with the length of the segments. (See Warner and Brickhill 1978 for an explanation of the periodogram technique and applications to visual pulsations from several dwarf novae.)

A more successful approach is illustrated in Figure 5, which is a three-dimensional "phase diagram" of a small portion of the data from the beginning of the observation. Each of the curves in the figure represents 128 s of data folded into 10 phase bins using an 8.76 s pulsation period, which was the best-fit period for the latter part of the observation. The curves are sequential with a 50% overlap. Three cycles of the fold are repeated in each curve to show more clearly the phase excursions about the mean period and the apparent amplitude changes.

We have used essentially the above method to derive the amplitude and phase of the pulsation as a function of time. A quantitative analysis of these parameters is presented in the next section. That this refinement over techniques used in analyzing the optical pulsations was possible is due to the large

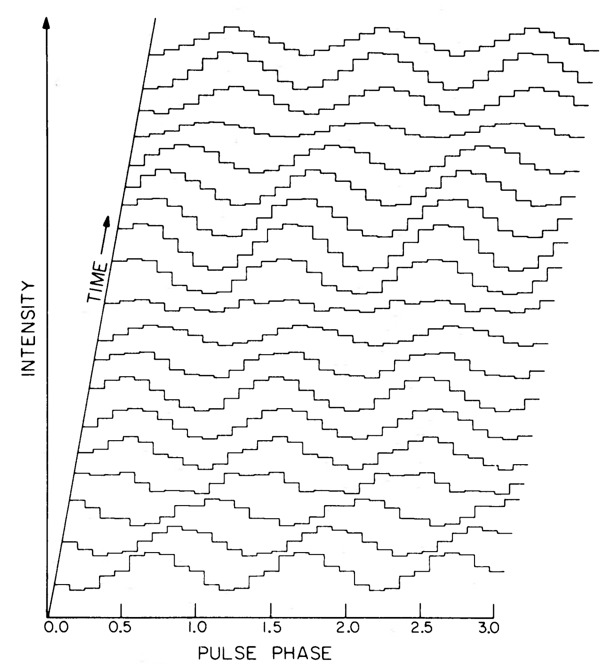

FIG. 5.—A phase diagram for a portion of the X-ray data illustrating the phase wanderings and large apparent changes in the pulsation amplitude. Each trace is a fold of 128 s of data at a period of 8.76 s. There is a 50% overlap between traces.

amplitude of the soft X-ray pulsations ($\sim 30\%$ as compared with $\lesssim 0.1\%$ in the visual).

III. DETAILED ANALYSIS OF THE PULSATION

We determine pulse arrival times by cross-correlating individual pulses or groups of pulses with a master pulse profile. For SS Cyg, the master pulse is a simple sinusoid, and hence the procedure reduces to fitting short segments of the data with a sinusoid, obtaining the amplitude and phase of the pulsation. These quantities are shown in Figure 6 from a fit to every independent set of four consecutive pulses (28 bins of 1.28 s each) in each orbit. We have similarly fitted sets of individual pulses and, separately, sets of up to 10 consecutive pulses, obtaining nearly identical results.

An important point must be appreciated with regard to the phase of the pulsations. Whenever the amplitude of the pulsation becomes small enough to be comparable to the uncertainty in the determination of the amplitude, the phase of the pulsation becomes undefined. We wish to obtain a set of arrival times that are well enough defined so that a statistical analysis will give reliable results. Thus we must consider only those points for which the amplitude is nonzero at a high enough confidence level to be sure that less than one arrival time in our set is expected to be spurious. We have used a *cutoff* at the 99.0% confidence level to ensure that this will be true in the set of 209 arrival times shown in Figure 6*b*, which represents 72% of the data.

An outstanding characteristic of Figure 6 is the independence of the amplitude and phase variations. The amplitude can change by a factor of ~ 6 within ~ 15 pulses with no effect on the pulse phase (e.g., see the middle of OB3). The pulse phase exhibits both slow variations and rapid jumps. Near the end of OB1 the phase jumps by $134° \pm 26°$ ($1\ \sigma$) from one group of four cycles to the next group with no effect on the amplitude. Also, in the middle of OB2, there is a phase jump of $234° \pm 24°$ from one set of four cycles to another set separated by three sets not shown in the figure. The phases of those sets were $24° \pm 24°$, $101° \pm 32°$, and $197° \pm 24°$, which implies a phase change of $173° \pm 34°$ within ~ 10 pulse cycles. (The amplitudes of these sets were nonzero by more than $1\ \sigma$. Thus less than one phase is expected to be spurious in this set of three phases.) Note that the rapid rise in amplitude occurs *after* this phase shift.

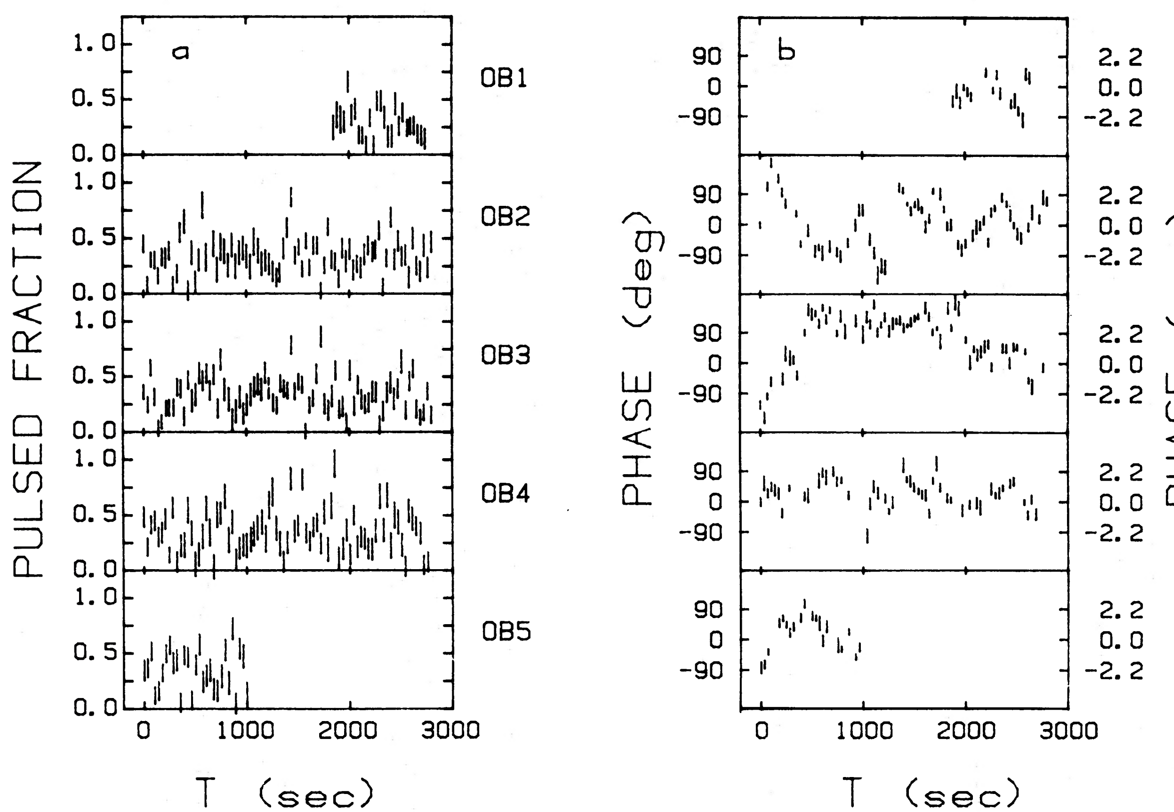

FIG. 6.—(*a*) The pulsed amplitude for every set of four consecutive pulse periods, in units of the average count rate from SS Cyg for each orbit, plotted versus a reference time near the beginning of each spacecraft orbit. Counting statistics introduces a noise amplitude of ~ 0.14. (*b*) The time delay (or phase) of each arrival time relative to a constant period plotted versus time in the same way as in (*a*). Only points that are significant at the 99% level are shown. The periods used were 8.893, 8.876, 8.785, 8.757, and 8.745 s, respectively. Positive residuals imply tardy pulses.

Examination of *individual* pulses does not yield any further information on the jumps except for their probable sign, because of the larger uncertainties in the individual pulse quantities.

The mean pulsed fraction of the source is $\sim 30\%$. (The mean determined from Fig. 6*a* includes noise from counting statistics, which increases that mean to 0.34.) Amplitude variability is present; for each orbit, the reduced χ^2 about a constant value is ~ 4. Thus the intrinsic variability in the pulsed fraction is roughly twice the observational error.

The distribution of pulsation amplitudes, employing two different definitions of pulsed fraction, is shown in Figure 7. Consider a pulse $A + B\cos(\omega t)$. In Figure 7*a*, as in Figure 6*a*, the pulsed fraction for each pulse is defined as $B/\langle A\rangle$, where $\langle A\rangle$ is the mean intensity for the entire OB containing that pulse. Thus this figure reflects the *pulsed amplitude* distribution of all pulses, since the mean intensity acts only as an overall normalizing factor. In Figure 7*b*, the pulsed fraction is defined as B/A. Hence this figure reflects the *pulsed fraction* distribution. [Recall that the pulsed fraction so defined ranges between 0 and 200%; a pulse $1 + \cos(\omega t)$ has a pulsed fraction of 100%, whereas a δ function, which equals $1 + 2\cos(\omega t) + \cdots$, has a pulsed fraction of 200%.] For example, if $B \propto A$, with A variable, Figure 7*a* would give the distribution of A, whereas all the pulses in Figure 7*b* would fall in the same pulsed fraction bin, B/A. The similarity of the two distributions testifies to the constancy of the mean intensity of SS Cyg and the true variability of the pulsed fraction, which ranges from ~ 0 to $\sim 100\%$. (Examination of the individual pulses with pulsed fractions over 100% shows that they are all consistent with a pulsed fraction of 100% within measurement errors.) Note that the mean of both histograms is now 44% due to the increased noise amplitude, which is $\sim 28\%$ for a fit to individual pulses.

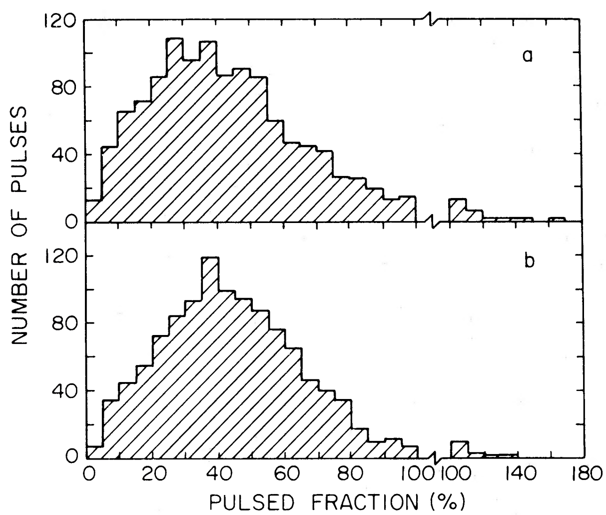

FIG. 7.—Two forms of the amplitude distribution of single pulses. (*a*) The pulsed fraction is here defined as the ratio of the pulsed amplitude for each pulse to the mean intensity for the entire OB containing that pulse. All 1166 pulses are displayed. (*b*) The pulsed fraction is here defined as the ratio of the pulsed amplitude for each pulse to the mean intensity determined during each pulse. The 4% of all pulses with mean intensities less than approximately half the mean intensity for each OB are excluded because of the large uncertainty in their pulsed fraction. (Note the *x*-axis scale change at a pulsed fraction of 100%.)

The magnitude of the phase variability prevents connecting the phase of the pulsation between OBs. Hence the binary orbital time delay with an expected amplitude of ~ 1.5 s (Walker and Chincarini 1968) cannot be seen. However, there is no ambiguity in pulse numbering within each orbit except for the two large phase jumps noted above.

This phase variability is also evident in the distribution of χ^2 values obtained in fitting a constant plus sinusoid to every group of n pulses. Although the observed χ^2 distribution closely resembles the expected χ^2 distribution for $n = 1$ or 2, it deviates noticeably from the expected χ^2 distribution as n increases.

In attempting to fit short stretches of the arrival times with a constant period, a poor fit is obtained in general. That is, an intrinsic uncertainty in the arrival times must be (quadratically) added to the measured uncertainties in order to obtain a fit with a reduced χ^2 of unity. Following this procedure, we show in Figure 8*a* how the period varies with time on short time scales. We have chosen time intervals in such a way as to show the full range of variability of the period. In Figure 8*b*, the period and its uncertainty as derived from each orbit of data are given by the solid error bars. The period shows an irregular general decrease, to be discussed further below.

The noise properties of the phase of the oscillation can be investigated by examining how the variance of the phase about a constant period depends on time. We do this in the following way. Consider all sets of arrival times spanning n pulse periods. We determine the best-fit period and the intrinsic uncertainty for each set as detailed above. From all these sets, we obtain a mean intrinsic uncertainty $\sigma_{\rm int}$ and its standard deviation, taking into account the degree of dependence of the overlapping sets. Figure 9 shows how $\sigma_{\rm int}^2$ depends on n. In interpreting Figure 9, be aware that each point is partially dependent on its neighbors.

The variance increases approximately linearly with time, which is consistent with a *random walk in phase caused by white noise in the period of the oscillation.* Although meaningful statistical estimates of $\sigma_{\rm int}$ cannot be made for time intervals longer than those shown in Figure 9, point estimates are available from the entire length of each satellite orbit. From OB1 and 5 ($n \sim 100$), $\sigma_{\rm int}$ equals 36° and 54°, and from OB2, 3, and 4 ($n \sim 300$), $\sigma_{\rm int}$ equals 69°, 78°, and 37°. These estimates are consistent with the extrapolation of Figure 9. It is important to note that all these estimates of $\sigma_{\rm int}$ are *lower bounds* to the true variance in the data because the period that was fitted to each stretch absorbed a large portion of the variance.

To determine the strength of the random walk, we construct artificial data and analyze the data in the

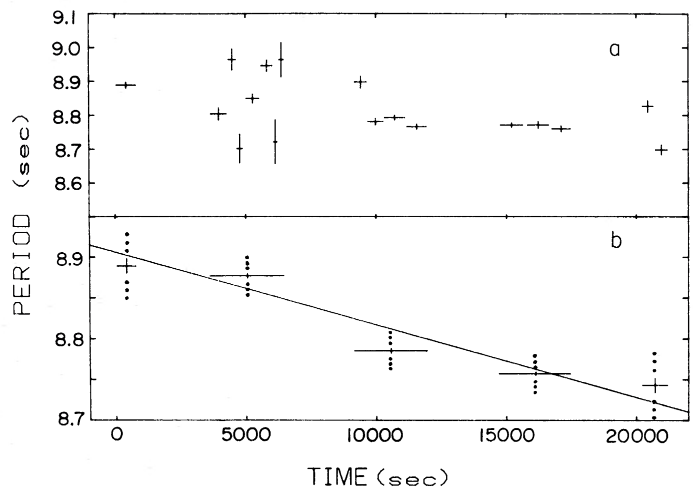

FIG. 8.—(*a*) The period of the oscillation plotted as a function of time as determined from short sections of the data. (*b*) The period for each orbit plotted as a function of time. The solid error bars give the formal errors, and the dotted error bars give errors derived from artificial data assuming a random walk.

same fashion as above. Let $\{T_N\}$ be a set of arrival times generated by $T_N = T_{N-1} + P_N$, where $P_N = P_0 + P_1 x_N$, P_0 and P_1 are fixed numbers, and x is a normally distributed random variable with a mean of zero and unit standard deviation. An "observational uncertainty" was assigned to these times by utilizing the actual measurement errors of the real data. For $P_0 = 8.77$ s, we find that $P_1 = 0.44 \pm 0.06$ s produces a curve consistent with Figure 9.

The artificial data closely resemble the observed arrival times. We show in Figure 10 the first set of random data produced using the above values of P_0 and P_1. The "structure" of the data in Figure 10 is strikingly similar to that of Figure 6*b*. In both figures the period appears to assume several discrete values with sudden transitions between periods; a few large phase jumps are also present. There have been several reports in the literature of multiple periods or erratic shifts in the optical oscillations from dwarf novae (Robinson 1973; Warner and Brickhill 1978). The

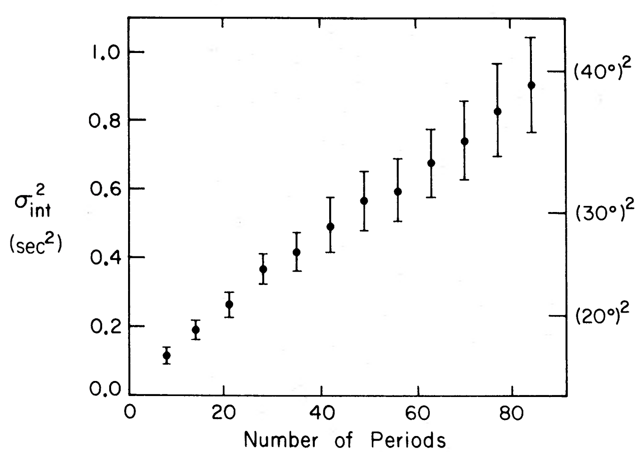

FIG. 9.—The mean intrinsic variance derived from all sets of arrival times spanning n periods plotted versus n.

evidence in Figure 10 suggests that both these effects may be due to a random-walk noise process.

Although we know that phase steps must occur at least as often as once per cycle, we do not know the true frequency of the steps. Thus, instead of specific values of P_0 and P_1, our simulation gives us the strength of the random walk, which is defined as a rate of phase steps times the mean square phase step:

$$S = R\langle(\Delta\phi)^2\rangle = \frac{1}{P_0}\left(\frac{2\pi P_1}{P_0}\right)^2 = 0.011 \pm 0.003 \text{ s}^{-1}. \quad (1)$$

This strength is just the slope of the phase variance versus time relation that would be found if the generating period P_0 were known. In a random walk of this strength, *the phase of the oscillation changes by 90° on the average every 25 ± 7 pulses!*

As noted before, however, the full variability implied by this strength of random walk is not seen directly in the data because the "true" period of the oscillation is unknown. Allowing the period to be a free parameter (as was done for Fig. 9) reduces the variance by a factor of ~7 for the case of SS Cyg. This makes the pulsation seem more coherent than it actually is. Thus the apparent mean square phase change is 90° only after ~175 cycles. (Note that the $\sigma_{\rm int}$ given in Fig. 9 is the average over a data set, and equals half the mean excursion from the first to last point.) Because the variance increases linearly with time, an apparent mean square phase change of 180° occurs only after ~700 cycles. This high apparent stability can account for the coherency previously attributed to the optical pulsations.

Our artificial data allow us to estimate the period variation caused by the random walk. For time intervals similar to OB1 and 5, the period uncertainty is ~0.05 s; for OB2, 3, and 4 it is ~0.03 s. These period uncertainties are ~10 times larger than the formally derived uncertainties in the periods for each

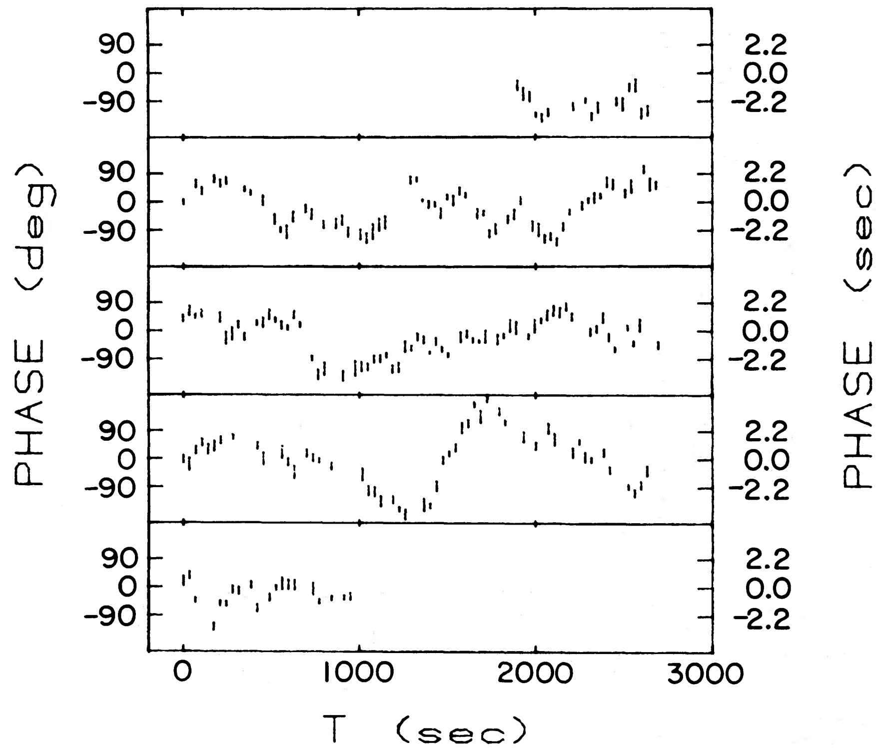

FIG. 10.—The time delay relative to a constant period of every fourth artificial pulse arrival time plotted versus time for $P_0 = 8.77$ s and $P_1 = 0.44$ s (see text). Uncertainties were taken from Fig. 6*b*. The periods found were 8.82, 8.71, 8.76, 8.78, and 8.79 s, respectively.

orbit, and are shown as the dotted error bars in Figure 8*b*.

We can now understand the erratic period shifts shown in Figure 8 as due to the random walk. Furthermore, any possible long-term period change can now be meaningfully determined. Using the period uncertainties given by the random walk and the best-fit periods for each OB, we find the following: (1) a fit to a constant period gives $P = 8.811$ s and $\chi^2 = 13.2$ with 4 degrees of freedom, with a probability of only 0.01 that this is a good fit; (2) a fit to a constant period $P = 8.88$ s for OB1–2 and a different constant period $P = 8.76$ s for OB3–5 yields $\chi^2 = 1.3$ with 3 degrees of freedom, and thus this interpretation cannot be ruled out; and (3) a fit to P and $\dot{P}$ yields $P = (8.906 \pm 0.031)\ \mathrm{s} - (8.9 \pm 2.6) \times 10^{-6} t$ (single parameter 1 σ errors), where t is measured from the beginning of OB1 and $\chi^2 = 1.2$ with 3 degrees of freedom. An F-test confirms that $\dot{P}$ is significant at the 99.0% confidence level. The result of the latter fit is shown in Figure 8*b* as a solid line.

If a random walk in *period* were also present, the phase variance found using the true period would equal $St + S't^3$. A firm upper limit to S' can be obtained by requiring that the contribution of the term in S' be less than the contribution of the term in S to the last point in Figure 9. This gives $S' < 10^{-8}\ \mathrm{s}^{-3}$. (If $S' = 10^{-8}\ \mathrm{s}^{-3}$, σ_{int} would be $\sim 300°$ for time intervals of 300 periods; this is much greater than the point estimates from OB2, 3, and 4.)

IV. DISCUSSION

a) *General*

The discovery of a 9 s pulsation in the soft X-rays from SS Cygni confirms the general expectation that high-energy pulsations are the ultimate source of the optical pulsations observed during outbursts of dwarf novae (Bath 1973; Warner and Brickhill 1978; Paczyński 1978). It is interesting that the origin of the pulsation is in soft X-rays, rather than hard X-rays. (In fact, hard X-rays were observed simultaneously during this pointing but no rapid periodicity was detected at the 6% level; Swank 1979.) Although the X-ray pulsed fraction was expected to be larger than the optical pulsed fraction, the large pulsation amplitude actually observed is perhaps surprising. The direct implication is that the pulsation cannot be merely a small perturbation of the X-ray source; it is instead an intrinsic part of the X-ray production mechanism.

The large pulsation amplitude also makes the near absence of harmonics in the pulse profile all the more surprising. Although the sinusoidal nature of the optical pulsations from dwarf novae had been emphasized before, Papaloizou and Pringle (1978) have pointed out that optical harmonics would be suppressed by the strong optical flickering and perhaps by smoothing if the optical light is reflected off the disk. Neither of these mechanisms affects the X-ray pulse profile. Thus this almost featureless pulse profile may constrain models for the pulsation.

Because of the high energies required to produce soft X-rays and the shortness of the pulsation period, it is probable that these X-ray observations probe the region near the compact star's surface. We can calculate a characteristic area of X-ray emission from the observed flux if we assume that the source emits a blackbody spectrum,

$$A = \frac{L}{\sigma T^4} \approx 2 \times 10^{15}\left(\frac{d}{200\ \mathrm{pc}}\right)^2\left(\frac{30\ \mathrm{eV}}{kT}\right)^4 \mathrm{cm}^2 . \quad (2)$$

The radiating area is much smaller than the area of a white-dwarf surface ($\sim 3 \times 10^{18}$ cm^2).

To derive a characteristic size for the radiating region, we can model the source area in two ways. If the X-rays come from a hot spot in the disk with $A = 2\pi R^2$, similar to the model proposed by Bath (1973),

$$R \approx 2 \times 10^7\left(\frac{d}{200\ \mathrm{pc}}\right)\left(\frac{30\ \mathrm{eV}}{kT}\right)^2 \mathrm{cm} . \quad (3)$$

An upper limit on the temperature of the remaining part of the ring of the disk containing the spot can be set by demanding that this ring contribute less X-ray luminosity ($E > 0.15$ keV) than the spot. This implies $T < \frac{1}{2}T_{\mathrm{spot}}$, assuming thermal emission. Thus, in this model the spot has a temperature enhancement by at least a factor of 2.

Alternatively, a radiating ring close to the degenerate star of area $2 \times 2\pi R_{\mathrm{WD}}\Delta R$ must have

$$\Delta R \approx 3 \times 10^5\left(\frac{d}{200\ \mathrm{pc}}\right)^2\left(\frac{30\ \mathrm{eV}}{kT}\right)^4\left(\frac{5 \times 10^8\ \mathrm{cm}}{R_{\mathrm{WD}}}\right) \mathrm{cm} . \quad (4)$$

This is about the thickness calculated for an optically thick boundary layer where the accreting disk material settles on the white dwarf surface (Pringle 1977).

We summarize below the characteristics of the X-ray pulsation:

(1) The pulsation is strong only during optical outbursts.
(2) The period is 9 s, and $\dot{P} \sim -1 \times 10^{-5}$ s s^{-1}.
(3) The phase apparently random walks, with $Q \sim 25$.
(4) The pulse profile is closely sinusoidal and of large amplitude (mean amplitude $\sim 30\%$, but individual pulsed fractions vary from 0 to 100%).
(5) The pulsation comes from a region of typical size 1–100 km with a temperature of ~ 30 eV and a total luminosity of $\sim 10^{33}$ ergs s^{-1}.

Optical pulsations sharing some of the above properties (1), (2), and (4) but with a much smaller amplitude have been observed in about 20 cataclysmic variable systems (Patterson, Robinson, and Nather 1977; Warner and Brickhill 1978; references in both). In fact, optical oscillations have been detected in SS Cyg itself during two different outbursts (neither of which corresponds to the outburst reported here). Patterson, Robinson, and Kiplinger (1978) recently reported a period of 9.7 s for SS Cyg. The pulsation amplitude was 0.02% when the system was at $V =$ 8.5 mag. For a different SS Cyg outburst, Horne and Gomer (1979) measured a pulsation period of 8.5 s and an amplitude $\sim 0.05\%$ for the system at 8.2 mag. Several days later, when the visual brightness had decreased to 9.6 mag, Patterson (1979) measured a pulsation period of 10.6 s and an amplitude of $\sim 0.1\%$. Upper limits (90% confidence) to the optical pulsation amplitude during the 1978 June outburst reported here are 0.05% for June 12.4 UT (Stiening and Hildebrand 1978), and 0.1% for June 14.3 UT from our own observations.

The estimates of the X-ray flux and pulsed fraction of SS Cyg yield an upper limit to the optical pulsation amplitude that could be due to reprocessed X-ray pulsation. The soft X-ray flux listed in Table 1 is the flux at the Earth in the energy band 0.13–0.48 keV; when corrected for absorption and extrapolated over all frequencies, the total flux is $\sim 4.5 \times 10^{-10}$ ergs cm^{-2} s^{-1}, of which $\sim 30\%$ is pulsed. The ratio, then, of the flux in the high-energy pulsed component to the observed optical flux in the band 3400–6000 Å is ~ 1–2%. This is an order of magnitude greater than the maximum reported optical pulsation amplitude.

The direct contribution of the pulsed 30 eV blackbody spectrum to visible light is $\sim 3 \times 10^{-13}$ ergs cm^{-2} s^{-1} (3400–6000 Å). We estimate from the optical observations quoted above that the *maximum* energy in the visual pulsation is ~ 1–2×10^{-12} ergs cm^{-2} s^{-1}. Thus the possibility that the X-ray and optical pulsation come from different portions of the same ~ 30 eV spectrum cannot definitely be ruled out. A clear test of this would be either *multicolor* optical pulsation observations throughout the outburst and/or simultaneous X-ray/optical pulsation observations.

A possible correlation between the pulsation period and optical luminosity has emerged from the optical observations of a few dwarf novae in outbursts: near the beginning of the outburst the optical pulsation period decreases until it reaches a minimum at, or just after, the peak visual brightness (e.g., Patterson, Robinson, and Nather 1977). Then the period may increase throughout the decline to visual minimum. The X-ray period of SS Cyg is observed to decrease at peak visual light, yet the X-ray intensity may also be steadily decreasing. More observations are required to investigate any period/X-ray brightness correlation.

The most striking characteristic of the X-ray pulsations is their simultaneous phase incoherence and period stability. Superposed on the long-term period drift is a random walk in phase. That is, the pulsation does not remember where its *phase* should be on any time scale, yet it knows very well what its *period* should be. This property and the fact that 9 s is approximately the Keplerian period of matter orbiting near the surface of a 1 $M_{\odot}$ white dwarf give strong evidence that the X-ray pulsation period is connected to that Keplerian period. The phase incoherence may then be connected to the growth and decay times of disturbances in the orbiting matter.

Before considering possible models for the pulsation, we note that Robinson and Nather (1979) have proposed that there are two distinct types of pulsation seen in cataclysmic variables: "coherent" oscillations claimed to have *phase coherence* but otherwise having the properties discussed above, and "quasi-periodic" oscillations with *phase incoherence*, longer periods, a broad range of simultaneously excited periods, and no evidence of long-term period stability. Obviously, the observed phase incoherence of the X-rays from SS Cyg, *which otherwise fall into the "coherent" pulsation class*, forces a reanalysis of the basis of the classification. (Note how Fig. 8 of Patterson, Robinson, and Nather 1977, which shows how the variance of the *quasi-periodic* oscillation in the dwarf nova RU Peg grows in time, resembles our Fig. 9.) While two classes of pulsation may still exist, our analysis points to the need for quantitative observational estimates of the degree of coherence of *all* the observed periodicities in cataclysmic variables.

b) The Nature and Origin of the X-Ray Oscillations

The low Q of the X-ray pulsations excludes a magnetic rotator model or any pulsation of the entire white dwarf. It seems most likely that the observed oscillations are due to pulsation instabilities. There are three regions that may be subject to such instabilities: the surface layers of the white dwarf, the boundary layer between the white dwarf and the accretion disk, and the accretion disk itself.

Papaloizou and Pringle (1978, hereafter PAP) have investigated the modes of a rotating pulsing star and find that either toroidal "r" modes concentrated in the white-dwarf surface layer, or g modes modified to originate in a rotating surface layer, may produce the observed optical pulsations. The periods of these modes are of order $1/m$ times the rotation period of the outer layers of the white dwarf (m is the azimuthal wavenumber). For any theory to be able to produce the large amplitude X-ray pulsations, m must be small. At the time PAP's theory was proposed, it was thought that the phase of the pulsation was as coherent as the period of the pulsation, i.e., $Q \sim 10^5$. This would be expected in any model that depends on the rotation of a white-dwarf surface layer, which contains a substantial amount of material. The Q of ~ 25 measured in this observation implies that a region of very small inertia must be responsible for the emission.

Therefore, we propose that the instability arises in the boundary layer or the inner disk. Most of the accretion energy will be dissipated where the velocity gradient is largest, i.e., in the outer portion of the boundary layer. The temperature of the X-ray source measured for SS Cyg (3×10^5 K) is approximately that predicted for a heated, optically thick boundary layer (Pringle 1977). The pulsation mechanism must depend on the stability and properties of the mass flow. The mechanism must produce almost sinusoidal pulsations whose amplitude and phase can suffer sudden, and apparently random, changes.

In the theory of boundary layers of the type usually considered in fluid mechanics, there exist instabilities which have the above properties (e.g., see reviews by Morkovin 1958; Roshko 1976). The theory is complicated, owing to the nonlinear processes it attempts to describe, and only very simple laboratory experiments have been attempted to demonstrate the existence of these instabilities (Schlichting 1968; Greenspan 1968). The instabilities can manifest themselves as sinusoidal oscillations whose coherence is a function of the shear flow parameters. Although the boundary layers considered in these references are quite different from the one we consider, we merely wish to point out that such instabilities are not unprecedented.

There are many ways in which the boundary layer could give rise to pulsed X-rays, which can be broadly classified into nonradial and radial instabilities. Consider first the nonradial instabilities. One type of instability which has been discussed in relation to cataclysmic variables is the Kelvin-Helmholtz instability. PAP point out that the interaction at the boundary layer may allow a nonlinear cycle of a quasi-coherent nature. Alternatively, oblique shocks in the boundary layer may produce the X-rays. The shocks probably have lifetimes of only a few pulses or less, and hence can easily give phase incoherence. Finally, the presence of the boundary layer gives rise to a region where the angular velocity of material rotating in the disk/boundary layer reaches a maximum. It is possible that an unstable density wave trapped in this region produces the X-ray pulsation. The dispersive properties of this wave may then account for the phase instability. These waves might even be the agent allowing matter to accrete onto the white dwarf.

Radial pulsation models in the boundary layer are also viable because the radial pulsation periods are close to the Keplerian periods at the outer edge of the boundary layer (Novikov and Thorne 1973). A variation in the boundary layer thickness, in either the radial or the axial direction or both, would necessarily affect the X-ray production. If, for example, either the stellar rotation axis or a stellar magnetic field axis were not aligned with the orbital angular momentum vector, a periodic radial push would be applied to the rotating matter. Alternatively, the boundary layer may itself be unstable to radial perturbations.

The disk itself may be the origin of the soft X-ray pulsations. Patterson, Robinson, and Nather (1977) and Robinson and Nather (1979) have proposed that the quasi-periodic optical oscillations, on the basis of their low coherence and relatively long periods, are an ubiquitous property of accretion disks. The pulsation may be triggered by an increased mass flux through the disk. Orbiting hot spots, oscillating rings, and spiral density waves have been suggested as possible physical mechanisms.

The development of these and other models will require much further theoretical work which we will not pursue here. However, we emphasize that if the pulsations are tied to the Keplerian period of matter rotating near the white dwarf surface, as we propose, *the pulsation period alone sets a lower limit on* $M_{\rm WD}/R_{\rm WD}^3$, *independent of the usual geometric unknowns* (such as the inclination of the binary system). Thus a theory which can compute how the observed pulsation period depends on the white-dwarf mass is of fundamental importance. Such a theory will be necessary to derive actual estimates of the white-dwarf mass because of the range of periods present in the boundary layer. As an illustration, *if* the observed X-ray pulsation period gives an upper limit to the Keplerian period at the white-dwarf surface, we find a mass for SS Cyg in excess of 0.9 $M_\odot$, using white-dwarf models given in Schwarzchild (1958). This speculative lower limit is consistent with the mass estimate of Kiplinger (1979).

In conclusion, none of the existing models for the optical pulsations correctly explains the X-ray oscillation behavior. The pulsations may arise from an as yet unspecified instability in the boundary layer or inner disk. The fact that this instability occurs for dwarf novae only in outburst, yet is observed to occur sporadically in other subclasses of cataclysmics that are in nonflaring states, indicates that a critical flow must be reached before these instabilities may occur. If this is true, then the coherence, amplitude, and pulse shape of the oscillations should also depend on the accretion flow parameters.

In support of this hypothesis, we also offer as evidence the detection of large amplitude X-ray pulsations of a quasi-periodic nature in U Geminorum on the decline from maximum ($P \sim$ 20–30 s; Córdova *et al.* 1980). Preliminary analysis suggests that the main difference between U Gem and SS Cyg is that the random walk is stronger in U Gem or, equivalently, a broader range of periods is simultaneously excited.

V. IMPLICATIONS FOR FUTURE OBSERVATIONS

It has proved difficult to develop theories of dwarf novae because of the many unknowns of the mass accretion process. Hence observations must play a fundamental role in guiding theory. Our results point to the need for the following observations of dwarf novae.

1) The soft X-ray light curve must be sampled over the entire outburst, especially near the beginning.

2) Other systems must be observed in X-rays to investigate the effects of the orbital inclination, $M_{\rm WD}$, and accretion rate.

3) More sensitive detectors must be employed to better define how sinusoidal the pulses are, and to test whether the X-ray spectrum changes during the pulse.

4) The coherence properties of *all* the observed pulsations (optical as well as X-ray) must be *quantitatively* investigated.

5) Optical observations must investigate the wavelength dependence of the pulsation amplitude in order to test whether the optical pulsation is the tail of the X-ray pulsation spectrum or whether it is reprocessed X-ray radiation. Simultaneous X-ray/optical observations could not only decide this question but may also constrain disk parameters if the optical pulsation is due to reprocessed X-ray radiation (Chester 1979).

It is hoped that the new insights gained from the X-ray observations will stimulate the development of theories that can fruitfully interact with observations. While it would be satisfying just to understand how the X-ray pulsation is produced, successful theories may allow the fundamental parameters of these interesting systems to be better defined.

We are indebted to Mr. J. Morgan for alerting us to the SS Cyg outburst. It gives us much pleasure to thank Ms. J. Mattei and the entire AAVSO for the simultaneous monitoring of this and many other cataclysmic variable stars. We are grateful to Dr. J. Swank, Mr. J. Aiello, Dr. S. Gull, Mr. J. Nugent, Dr. P. Szkody, and Ms. M. Conroy for their contributions to various aspects of the data acquisition and reduction, and to Ms. J. Boyer and Ms. D. Welch who prepared this manuscript for publication. Interesting discussions are acknowledged with Drs. R. Blandford, S. Weber, P. Goldreich, J. Nelson, and R. Wade. F. A. C. wishes to especially thank Drs. W. Priedhorsky and W. Krzeminski for pointing her in the direction of these fascinating stars. This work was supported by NASA contract NAS 5-25049 and by the National Science Foundation [AST 80801 A01].

REFERENCES

Bath, G. T. 1973, *Nature Phys. Sci.*, **246**, 84.
———. 1976, in *IAU Symposium No. 73, Structure and Evolution of Close Binary Systems*, ed. P. Eggleton, S. Mitton, and J. Whelan (Dordrecht: Reidel), p. 173.
———. 1978, *Quart. J.R.A.S.*, **19**, 442.
Brown, R. L., and Gould, R. J. 1970, *Phys. Rev. D*, **1**, 2252.
Chester, T. J. 1979, *Ap. J.*, **230**, 167.
Córdova, F. 1979, in *IAU Colloquium 53, White Dwarfs and Variable Degenerate Stars*, ed. H. Van Horn and V. Weidemann (Rochester: University of Rochester), in press.
Córdova, F. A., Chester, T. J., Garmire, G. P., Mason, K. O., and Kahn, S. M. 1980, in preparation.
Davidsen, A. F., Henry, R. C., Snyder, W. A., Friedman, H., Fritz, G., Naranan, S., Schulman, S., and Yentis, D. 1977, *Ap. J.*, **215**, 541.
Greenspan, H. P. 1968, *The Theory of Rotating Fluids* (London: Cambridge University Press).
Hearn, D. R., Richardson, J. A., and Li, F. K. 1976, *Bull. AAS*, **8**, 447.
Heise, J., Mewe, R., Brinkman, A. C., Gronenschild, E. H. B. M., den Boggende, A. J. F., Schrijver, J., Parsignault, D. R., and Grindlay, J. E. 1978, *Astr. Ap.*, **63**, L1.
Horne, K., and Gomer, R. 1979, *Ap. J.*, submitted.
Kellogg, E., Baldwin, J. R., and Koch, D. 1975, *Ap. J.*, **199**, 299.
Kiplinger, A. 1979, *A.J.*, **84**, 655.
Lampton, M., Margon, B., and Bowyer, S. 1976, *Ap. J.*, **208**, 177.
Margon, B., Szkody, P., Bowyer, S., Lampton, M., and Paresce, F. 1978, *Ap. J.*, **224**, 167.

Mason, K. O., Córdova, F. A., and Swank, J. H. 1979, *Proc. COSPAR Symposium*, Innsbruck, ed. W. A. Baity and L. E. Peterson (Oxford: Pergamon), in press.
Morkovin, M. V. 1958, *ASME Trans.*, **80**, 1121.
Novikov, I., and Thorne, K. S. 1973, in *Black Holes, Les Houches*, ed. C. DeWitt and B. S. de Witt (New York: Gordon & Breach), p. 344.
Paczyński, B. 1978, in *Nonstationary Evolution of Close Binaries*, ed. A. Zytkow (Warsaw: Polish Scientific Publishers), p. 89.
Papaloizou, J., and Pringle, J. E. 1978, *M.N.R.A.S.*, **182**, 423 (PAP).
Patterson, J. 1979, private communication.
Patterson, J., Robinson, E. L., and Kiplinger, A. L. 1978, *Ap. J. (Letters)*, **226**, L137.
Patterson, J., Robinson, E. L., and Nather, R. E. 1977, *Ap. J.*, **214**, 144.
Pringle, J. E. 1977, *M.N.R.A.S.*, **178**, 195.
Rappaport, S., Cash, W., Doxsey, R., McClintock, J., and Moore, G. 1974, *Ap. J. (Letters)*, **187**, L5.
Ricketts, M. J., King, A. R., and Raine, D. J. 1979, *M.N.R.A.S.*, **186**, 233.
Robinson, E. L. 1973, *Ap. J.*, **183**, 193.
———. 1976, *Ann. Rev. Astr. Ap.*, **14**, 119.
Robinson, E. L., and Nather, R. E. 1979, *Ap. J. Suppl.*, **39**, 461.
Roskho, A. 1976, *AIAA J*, **14**, 1349.
Rothschild, R., *et al.* 1979, *Space Sci. Instr.*, **4**, 269.
Schlichting, H. 1968, *Boundary Layer Theory* (New York: McGraw-Hill).
Schwarzchild, M. 1958, *Structure and Evolution of the Stars* (New York: Dover).
Stiening, R. F., and Hildebrand, R. 1978, private communication.
Swank, J. H. 1979, private communication.
Walker, M. F., and Chincarini, G. 1968, *Ap. J.*, **154**, 157.
Warner, B. 1976, in *IAU Symposium No. 73, Structure and Evolution of Close Binary Systems*, ed. P. Eggleton, S. Mitton, and J. Whelan (Dordrecht: Reidel), p. 85.
Warner, B., and Brickhill, A. J. 1978, *M.N.R.A.S.*, **182**, 777.

T. J. CHESTER: 1169 Meadowbrook Road, Altadena, CA 91001

F. A. CÓRDOVA: Los Alamos Scientific Laboratory, MS 436, Los Alamos, NM 87545

G. P. GARMIRE: Downs Laboratory of Physics, 320-47, California Institute of Technology, Pasadena, CA 91125

I. R. TUOHY: Research School of Physical Sciences, Australian National University, Canberra, Australia